

DAB2IP regulates the chemoresistance to pirarubicin and tumor recurrence of non-muscle invasive bladder cancer through STAT3/Twist1/P-glycoprotein signaling



Kaijie Wu^{a,1}, Bin Wang^{a,1}, Yule Chen^a, Jiancheng Zhou^a, Jun Huang^a, Ke Hui^a, Jin Zeng^a, Jianning Zhu^a, Kai Zhang^a, Lei Li^a, Peng Guo^a, Xinyang Wang^a, Jer-Tsong Hsieh^b, Dalin He^{a,*}, Jinhai Fan^{a,*}

^a Department of Urology, First Affiliated Hospital of Xi'an Jiaotong University, Xi'an 710061, PR China

^b Department of Urology, University of Texas Southwestern Medical Center, Dallas 75390, TX, USA

ARTICLE INFO

Article history:

Received 16 September 2015

Accepted 23 September 2015

Available online 26 September 2015

Keywords:

Bladder cancer

Pirarubicin

Tumor recurrence

DAB2IP

Twist1

P-glycoprotein

ABSTRACT

There is a high frequency of tumor recurrence in non-muscle invasive bladder cancer (NMIBC) after transurethral resection and postoperative intravesical chemotherapy, however, the molecular mechanisms leading to the chemoresistance and tumor re-growth remain largely unknown. In this study, we observed a significant decrease of DAB2IP expression in high-grade and recurrent NMIBC specimens, which was negatively correlated with Twist1 expression and predicted a lower recurrence-free survival of patients. Mechanistically, DAB2IP could inhibit the phosphorylation and transactivation of STAT3, and then subsequently suppress the expression of Twist1 and its target gene P-glycoprotein, both of which were crucial for the pirarubicin chemoresistance and tumor re-growth of bladder cancer cells. Overall, this study reveals a new promising biomarker modulating the chemoresistance and tumor recurrence of NMIBC after bladder preservation surgery.

© 2015 Elsevier Inc. All rights reserved.

1. Introduction

Bladder cancer (BCa) is one of the most common urological malignancies, and more than 70% of cases are non-muscle invasive bladder cancer (NMIBC) [1]. Transurethral resection (TUR) of bladder tumors followed by postoperative intravesical chemotherapy (i.e., pirarubicin) or Bacillus Calmette–Guérin (BCG) immunotherapy is the most efficient treatment for patients with NMIBC. However, there is a high propensity of tumor recurrence after bladder preservation therapy [2]. Drug-resistant cells are believed to be the main source of recurrent tumors after chemotherapy [3], however, the mechanisms contributing to chemoresistance and tumor recurrence of NMIBC remain largely unknown.

DAB2IP, a member of the RAS-GTPase activating protein (RAS-GAP) family [4], is down-regulated in multiple cancer types, including BCa. It has been reported that the promoter methylation of human DAB2IP gene occurred more frequently in muscle-invasive BCa (MIBC) than NMIBC [5]. Shen et al. also showed that DAB2IP loss was significantly

associated with high tumor stage and grade, and knocking-down DAB2IP in BCa cells could promote cell proliferation, migration and invasion as well as activation of the ERK and Akt pathways and induction of epithelial–mesenchymal transition (EMT) [6]. In consistency, our previous study also demonstrated that DAB2IP was significantly down-regulated in advanced or metastatic MIBC than NMIBC, and could predict a lower 3-year survival after radical cystectomy [7]. However, the potential roles of DAB2IP in NMIBC recurrence or progression have not been reported.

In this study, we further explored the expression of DAB2IP in NMIBC specimens with different pathological grades, especially in the recurrent tumors after TUR and intravesical pirarubicin instillation. Indeed, our data provide evidence to verify a decreased expression of DAB2IP in high-grade and recurrent NMIBC tissues. Mechanistically, we showed that DAB2IP could inhibit the phosphorylation and transactivation of signal transducer and activator of transcription 3 (STAT3), and then subsequently suppress the expression of Twist1, a basic helix–loop–helix transcription factor, and its target gene P-glycoprotein (P-gp), which were crucial for the chemoresistance to anthracyclines (i.e., pirarubicin) in BCa cells as demonstrated in our previous study [8]. Importantly, DAB2IP loss was correlated with Twist1 expression in BCa specimens, and indicated a lower recurrence-free survival of patients with NMIBC. Taken together, these results suggest that DAB2IP may be a promising biomarker to predict the prognosis of NMIBC.

* Corresponding author at: Department of Urology, First Affiliated Hospital of Xi'an Jiaotong University, #277 Yanta West Road, Xi'an 710061, PR China.

E-mail addresses: dalinhe@yahoo.com (D. He), jinhai029@126.com (J. Fan).

¹ K. Wu and B. Wang have contributed equally in this paper.

2. Materials and methods

2.1. Reagents and antibodies

Pirarubicin (THP), 3-(4,5-Dimethylthiazol-2-yl)-2,5-Diphenyltetrazolium Bromide (MTT) and Stattic (a specific STAT3 inhibitor) were obtained from Sigma-Aldrich Chemical (St. Louis, MO, USA). Antibodies used were as follows: anti-Twist1 (ab49254, Abcam, Cambridge, UK); anti-P-gp (sc-55510, Santa Cruz Biotechnology, Santa Cruz, CA, USA); anti-p-STAT3 (Tyr705, CST #9131, Cell Signaling Technology, Beverly, MA, USA); anti-STAT3 (sc-482, Santa Cruz Biotechnology); anti-GAPDH (sc-25778, Santa Cruz Biotechnology), and anti-DAB2IP, generated as described previously [9].

2.2. Cell line and cell culture

Human bladder cancer 5637 and 253J cell lines were kindly gifted by Dr. Leland W.K. Chung (Cedars-Sinai Medical Center, Los Angeles, CA, USA), and maintained in Dulbecco's modified Eagle's medium (DMEM, Gibco, San Diego, CA, USA) supplemented with 10% fetal bovine serum (FBS) at 37 °C with 5% CO₂ in a humidified incubator.

2.3. Plasmids and cell transfection

DAB2IP shRNA and its scrambled shRNA control, DAB2IP cDNA and its vector control, Twist1 siRNA and its scrambled siRNA control have been described in our previous studies [8,10]. The Twist1 reporter plasmid (Twist1-Luc) was kindly presented by Prof. Lu-Hai Wang (Mount Sinai School of Medicine, New York, NY, USA) [11]. STAT3 siRNA oligonucleotide (sequence: 5'-CACCGCAUCUCUACAUUCATT-3') and its scrambled siRNA control were designed and purchased from GenePharma (Shanghai, China). For shRNA, cDNA or siRNA transfection, 5 × 10⁵ cells were seeded in a 6-well plate (Costar, Lowell, MA, USA) with 70–80% confluence before transfection. The transfection was carried out using Lipofectamine LTX with PLUS (Invitrogen, Carlsbad, CA, USA) according to the manufacturer's instructions. 5637-luciferase cells were generated with a lentivirus system expressing a luciferase gene under selection of 400 µg/ml G418 for 2 weeks as described previously [12]. Stable 5637-luc transfectants with DAB2IP shRNA (i.e. 5637 KD) were selected in the complete medium containing 600 ng/ml Puromycin, and stable 253J transfectants with DAB2IP cDNA were selected in the complete medium containing 400 µg/ml G418.

2.4. Colony formation assay

A total of 5000 cells per well were seeded in 6-well plates for 24 h, and then switched into fresh medium containing 0.5 µg/ml THP for two weeks, and fresh medium was changed every 3–4 days. The plates were then washed with ice-cold PBS, fixed with 4% paraformaldehyde, stained in crystal violet solution for 15 min at room temperature and washed with distilled water to remove excess dye. The number of colonies was counted for each sample.

2.5. Cell viability assay

Cell viability was determined by MTT assay as previously described [8]. Briefly, cells were seeded into 96-well plates. After 24 h, the medium was changed by fresh medium containing various concentration of THP (0, 0.1, 1, 5, 10, 20 µg/ml) for another 24 h, followed by supplement of 20 µg MTT (5 mg/ml) for 4 h. Viable cells were detected by a 96-well microplate reader (Bio-Rad, Hercules, CA, USA) at a wavelength of 490 nm. The value of half-maximal inhibitory concentration (IC₅₀) to THP was calculated using linear regression analysis.

2.6. RNA extraction and quantitative RT-PCR

qRT-PCR was performed as described previously [13]. In brief, RNA was isolated using RNeasy Kit (Qiagen, Valencia, CA, USA) and reverse transcribed with RevertAid™ kit (MBI Fermentas, St. Leon-Rot, Germany) according to the manufacturer's instructions. cDNA was subjected to a 25 µl real-time PCR carried out in an iCycler thermal cycler (Bio-Rad, Hercules, CA, USA) using iQ SYBR Green Supermix (Bio-Rad) with the gene-specific primers: Twist1, F: 5'-GGAGTCCGCAGTCTTACG AG-3'; R: 5'-TCTGGAGACCTGGTAGAGG-3'; MDR1, F: 5'-GTGTCCGT GGATCACAAGCC-3'; R: 5'-GCGAGCCTGGTAGTCAATGC-3'; 18S, F: 5'-GGAATTGACGGAAGGGCACCACC-3'; R: 5'-GTGCAGCCCCGGACATCTAA GG-3'.

2.7. Protein extraction and western blot

Total cellular protein lysates were prepared with RIPA buffer [50 mM Tris (pH 8.0), 150 mM NaCl, 0.1% SDS, 1% NP40 and 0.5% sodium deoxycholate] containing proteinase inhibitors, 1% Cocktail and 1 mmol/l PMSF (Sigma, St. Louis, MO, USA). A total of 20–40 µg of protein was separated by 7–12% SDS-PAGE and transferred to nitrocellulose membranes. Following blocking with 5% skim milk in Tris-buffered saline with 0.1% Tween 20 (pH 7.6, TBST), the membranes were incubated with primary antibodies at room temperature for 1.5 h. After being washed with TBST, membranes were incubated with secondary antibodies coupled to horseradish peroxidase at room temperature for 1 h and visualized with an ECL chemiluminescent detection system (Pierce, Rockford, IL, USA). Loading differences were normalized using a monoclonal GAPDH antibody.

2.8. Dual-luciferase reporter assay

For the reporter gene assay, cells seeded in 24-well plates were transfected with 200 ng Twist1-luc reporter gene constructs or STAT3-responsive luciferase reporter plasmid pLucTKS3 and 1 ng of the pRL-SV40 Renilla luciferase construct (as an internal control). Cell extracts were prepared 48 h after transfection, and the luciferase activity was measured using the Dual-Luciferase Reporter Assay System (Promega) as described previously [13]. Relative luciferase activity is represented as mean ± SEM from each sample after normalizing with control (= 1).

2.9. Intravesical instillation xenograft models and THP treatment

Female athymic BALB/c nu/nu mice at the age of 4–6 weeks were used to establish the intravesical orthotopic animal model according to the protocols approved by the ethical committee of Xi'an Jiaotong University. In brief, mice were anesthetized and a 24-gauge catheter was inserted into the bladder through the urethra. 100 µl of 0.2% trypsin in 0.02% EDTA was infused and retained in the bladder for 30 min, and then 5 × 10⁶ 5637-luc sublines (i.e., 5637 KD and its control) in 100 µl medium mixed with Matrigel (1:1, v/v) was instilled into the bladder. After 3 days and 1 week, mice were anesthetized again and THP (30 mg/m²) was instilled into bladder with a 24-gauge catheter for 30 min, respectively. Subsequently, Bioluminescence imaging (BLI) was performed to detect the tumor burden with injection of 450 mg/kg D-luciferin substrate (Biosynth, Naperville, IL, USA) in PBS into anesthetized mice after 3 weeks.

2.10. Immunofluorescence (IF) staining

Cells were fixed in 4% paraformaldehyde for 15 min at room temperature and washed three times with PBS then permeabilized with ice-cold 100% methanol for 10 min. The slides were blocked in PBS containing 0.3% Triton-X100 and 5% normal donkey serum for 1 h at room temperature. Primary antibody was incubated for 1 h at room temperature. After washing with PBS, cells were incubated with secondary antibodies

for 45 min at room temperature. Finally, cells were counterstained with 4',6-diamidino-2-phenylindole (DAPI) before mounting.

2.11. Clinical tissue samples and immunohistochemical (IHC) staining

All the paraformaldehyde-fixed and paraffin-embedded primary NMIBC tissues ($n = 187$) were obtained from the Institute of Urology, Xi'an Jiaotong University. All the tissues were obtained from TUR between 2003 and 2012. Among these patients with primary NMIBC, 32 patients were detected with tumor recurrence during the formal intravesical THP instillation and follow-up, and received a second TUR in our department. The histopathology of the specimens was examined and classified by pathologists from First Affiliated Hospital of Xi'an Jiaotong University. All samples were used after written consent was obtained from the patients.

IHC was carried out with Dako Autostainer Plus system (Dako, Carpinteria, CA, USA) as described [14]. Briefly, sections were deparaffinized, rehydrated and subjected to antigen retrieval in citrate buffer (10 mM, pH 6.0) for 5 min, and then endogenous peroxidase and alkaline phosphatase activity were blocked with Dual Block for 10 min. The slides were then incubated overnight at 4°C with DAB2IP (1:75 dilutions), Twist1 (1:100 dilutions) and P-gp antibodies (1:150 dilutions). After washing, this was followed by incubation with EnVision secondary antibody for 30 min at room temperature. Signals were detected by adding substrate hydrogen peroxide using diaminobenzidine (DAB) as a chromogen followed by hematoxylin counterstaining. DAB2IP expression in human NMIBC tissues was evaluated according to the intensity of the staining (0, 1+, 2+ and 3+) and the percentages of positive cells, which was separated by 0 (0%), 1 (1% to 33%), 2 (34 to 66%) and 3 (67 to 100%). Finally, the staining result was considered higher expression (intensity 2 or 3 and percent category 2 or 3) or lower expression (intensity 0 or 1, or more but percent category 0 or 1). For each section, the total score was calculated by multiplying the scores of intensity and percentage.

2.12. Statistical analysis

All statistical analyses were performed using SPSS 15.0 (SPSS Inc., Chicago, IL, USA). Quantitative data were presented as mean \pm SEM, and the differences between two groups were compared by the 2-tailed Student's *t* test. For analyzing gene-expression profiling and correlation, human bladder cancer data set GSE13507 ($n = 256$) [15] was used. Processed data were downloaded from NCBI GEO, and log₂ data for individual probes were Z scored for plotting. Spearman's correlation between DAB2IP and Twist1 expression was calculated by Prism 5.0 (GraphPad Software, La Jolla, CA, USA). Among these 256 patients, the expression of DAB2IP in 103 cases of primary NMIBC and 23 cases of recurrent NMIBC was compared. Recurrence-free survival curves for 103 cases of primary NMIBC were plotted using Kaplan–Meier analysis. $P < 0.05$ was considered statistically significant.

3. Results

3.1. Down-regulated DAB2IP expression in high-grade and recurrent NMIBC specimens after intravesical THP instillation

We have showed the distinct expression patterns of DAB2IP in NMIBC different with MIBC tissues in our previous study [7]. Herein, our IHC data also revealed a significant decrease of DAB2IP staining in NMIBC tissues with a higher pathological grade, meanwhile a strong staining of DAB2IP was observed in the cytoplasm of normal urothelium (Fig. 1A–B, $P < 0.05$). Moreover, we found that lower DAB2IP expression was detected in the recurrent tumor tissues after intravesical THP instillation in the same patients with a second TUR, indicating that DAB2IP loss may be associated with the chemoresistance to THP and tumor recurrence of NMIBC (Fig. 1C, $P < 0.05$).

3.2. DAB2IP regulates the chemosensitivity of BCa cells to pirarubicin treatment

Indeed, utilizing both loss-of-function and gain-of-function strategies in 5637 and 253J cell lines with different sensitivities to THP as showed in our previous study, we found that knockdown of DAB2IP could dramatically enhance the colony formation of 5637 cells treated with THP (Fig. 2A, $P < 0.05$); meanwhile overexpression of DAB2IP abolished the survival advantage of 253J cells after THP treatment (Fig. 2B, $P < 0.05$). In consistency, DAB2IP could significantly modulate the IC₅₀ of 5637 and 253J cells to THP treatment accordingly (Fig. 2C, $P < 0.05$). Together, the data indicated that DAB2IP could regulate the chemosensitivity of BCa cells to pirarubicin in vitro.

3.3. DAB2IP loss increases Twist1/P-glycoprotein expression in BCa cells

Furthermore, we examined the potential changes of Twist1 and P-glycoprotein (P-gp) expression, which were shown to play an important role in the chemoresistance to anthracycline drugs in BCa in our previous study [8]. Indeed, as shown in Fig. 3A (left and middle panel), western blot and qPCR data clearly showed that the expression of Twist1 and P-gp protein and mRNA increased in 5637 cells after DAB2IP knockdown. Consistently, overexpression of DAB2IP in 253J cells could downregulate the expression levels of Twist1 and P-gp protein and mRNA (Fig. 3A, left and middle panel). Furthermore, a negative regulation of Twist1 promoter activity by DAB2IP was also detected in both 5637 and 253J cells, indicating that DAB2IP could suppress Twist1 gene transcription in BCa cells (Fig. 3A and B, right panel). Furthermore, we observed the decreased Twist1 and P-gp protein levels in DAB2IP-deficient 5637 KD cells after DAB2IP overexpression in a dose-dependent manner (Fig. 3C, left panel), which would lead to the suppression of IC₅₀ to THP treatment (Fig. 3C, right panel, $P < 0.05$). Also, Twist1 knockdown dramatically decreased P-gp protein expression and IC₅₀ to THP treatment in 5637 KD cells (Fig. 3D, $P < 0.05$). Therefore, DAB2IP could suppress Twist1 gene expression and then abolish P-gp expression and THP chemoresistance in BCa cells.

3.4. DAB2IP regulated Twist1/P-glycoprotein expression and chemosensitivity of BCa cells to pirarubicin through STAT3 signaling

STAT3 has been shown to directly regulate Twist1 gene transcription [16], so we suppose that STAT3 may mediate the suppression of Twist1 expression by DAB2IP, because our previous study has demonstrated that DAB2IP could directly bind to and inactivate STAT3 activity [17]. Indeed, as shown in Fig. 4A, the expression of phosphorylated-STAT3 (p-STAT3) at tyrosine 705 (Y705) increased in 5637 cells after DAB2IP knockdown, while lower level of p-STAT3 (Y705) expression was detected in DAB2IP-overexpressing 253J cells. Moreover, more nuclear location of STAT3 was observed in 5637 cells after DAB2IP knockdown (Fig. 4B). To be consistent, using a specific STAT3-responsive luciferase reporter, we found that DAB2IP could modulate the transcription activity of STAT3. Because the elevated STAT3-responsive luciferase activity was detected in DAB2IP-deficient 5637 cells; while overexpression of DAB2IP in 253J cells could significantly suppress the STAT3-responsive luciferase activity (Fig. 4C, $P < 0.05$). Furthermore, we applied the STAT3 specific siRNA or inhibitor (i.e., Stattic) to knockdown STAT3 expression or inhibit STAT3 activity, and found that Twist1/P-gp protein expression and the IC₅₀ to THP treatment dramatically decreased in 5637 KD cells (Fig. 4D–E, $P < 0.05$). All the data support that DAB2IP regulated STAT3 phosphorylation, nuclear translocation and transcription activity, and then suppressed Twist1/P-gp expression and modulated the chemosensitivity of BCa cells to pirarubicin.

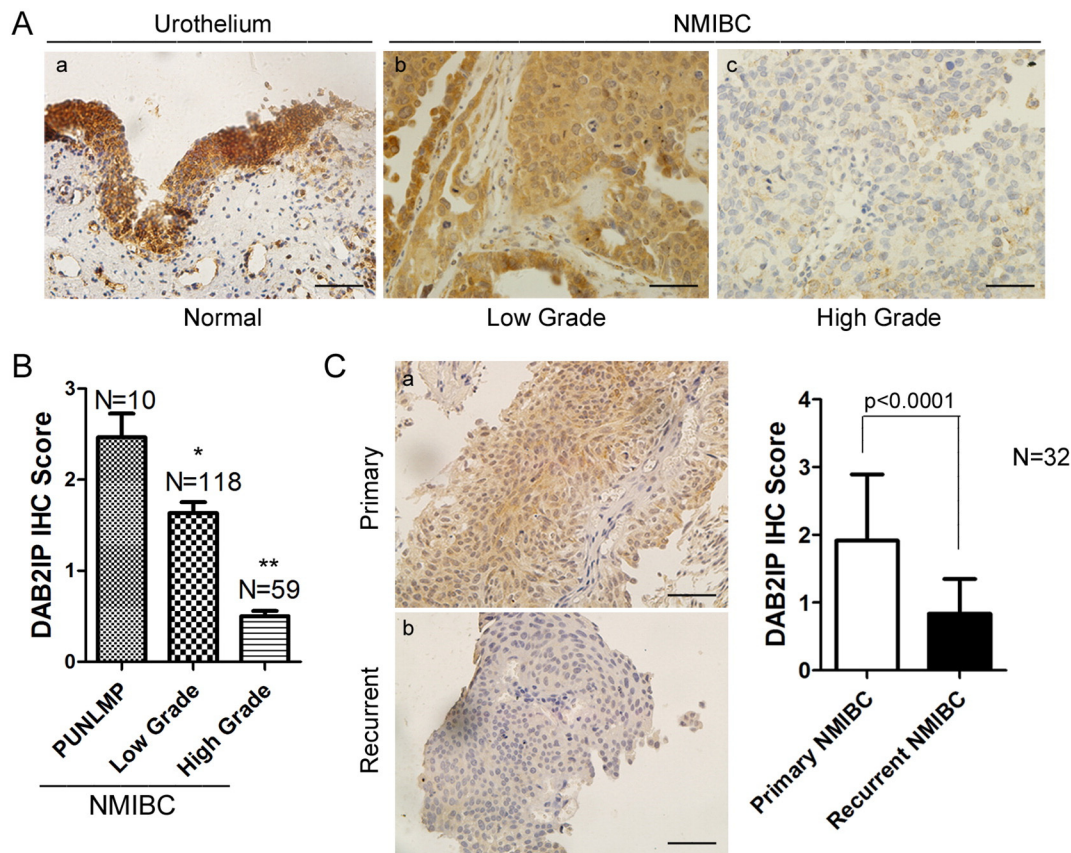


Fig. 1. Down-regulated DAB2IP expression in high-grade and recurrent NMIBC specimens after intravesical THP instillation. A, representative pictures of immunohistochemistry of DAB2IP in normal urothelial mucosa (a) or NMIBC tissues (b, c) with different pathological stages were shown, respectively. The scale bar represents 25 μm . B, quantification analysis of DAB2IP staining in NMIBC tissues with different pathological stages was shown (N = 187). Papillary urothelial neoplasm of low malignant potential (PUNLMP, N = 10), Low Grade (N = 118), High Grade (N = 59). * $P < 0.05$ vs. PUNLMP, ** $P < 0.05$ vs. Low Grade. C, representative pictures of immunohistochemistry of DAB2IP in primary (a) or recurrent (b) NMIBC tissues in the same patients after intravesical THP instillation were shown, respectively (left panel). The scale bar represents 25 μm . Right panel, quantification analysis of DAB2IP staining between primary and recurrent NMIBC tissues in the same patients (N = 32) was shown.

3.5. DAB2IP loss increases the *in vivo* orthotopic tumor growth after intravesical THP treatment

We further established the orthotopic xenograft tumors of 5637 sublines and tested their chemosensitivity to intravesical THP treatment. Indeed, we observed that knocking-down DAB2IP in 5637 cells could significantly enhance *in vivo* tumor growth after intravesical THP instillation. As shown in Fig. 5A, higher light units of tumors were observed in mice injected with 5637 KD cells, and quantity analyses revealed a significant increase of tumor burden compared to control cells (Fig. 5B, $P = 0.0012$). Also, we compared the expressions of Twist1 and P-gp in the xenograft tissues of 5637 sublines by IHC staining. In consistent with our *in vitro* observation, 5637 KD tumors presented a higher percentage of Twist1 and P-gp staining compared to control cells (Fig. 5C, $P < 0.05$). All these indicated that DAB2IP loss increased the *in vivo* orthotopic tumor growth after intravesical THP treatment, which may contribute to the tumor recurrence of NMIBC after intravesical chemotherapy.

3.6. DAB2IP is inversely correlated with Twist1 expression in NMIBC specimens and predicts the prognosis of patients

We also utilized our clinical samples to strengthen my finding in cell lines and xenografts. Indeed, we found that there was a negative correlation between DAB2IP and Twist1 expression in our NMIBC tumor tissues ($P = 0.007$, $R = -0.598$; representative pictures as shown in Fig. 6A), which was also supported by other microarray data (GSE13507) from NCBI GEO [15,18] (Fig. 6B, $P = 0.002$, $R = -0.224$).

Moreover, we analyzed the potential difference of DAB2IP mRNA expression levels between primary and recurrent NMIBC specimens in this cohort, and found that lower DAB2IP mRNA was expressed in the recurrent NMIBC tissues (Fig. 6C, $P = 0.0001$). Also, we further found a significant association between DAB2IP mRNA level and recurrence-free survival of patients with NMIBC. The patients with a lower DAB2IP expression had a poor prognosis with a lower recurrence-free survival (Fig. 6D, $P = 0.0018$). This data indicated that decreased DAB2IP expression was correlated with higher Twist1 expression and could predict tumor recurrence of patients with NMIBC.

4. Discussion

Bca is a heterogeneous and unpredictable disease, in which NMIBC has a relative high recurrence rate but a low progression rate. Several risk assessment calculators based on the clinicopathological parameters (i.e., EORTC risk score) are developed for NMIBC to evaluate the tumor recurrence and progression after TUR and postoperative intravesical therapies. However, they may have defects and more precise risk stratification is required [19]. Recently, molecular markers (i.e., p53, survivin) have proved their prognostic or predictive value in NMIBC, and may improve the risk stratification for both recurrence and progression of NMIBC [20,21]. Therefore, to explore more novel markers for distinguishing the high-risk NMIBC is crucial to evaluate the patient prognosis and treatment options.

DAB2IP, also named ASK1-interacting protein 1 (AIP1), is a new member of the RAS-GAP family that acts as a tumor suppressor gene. It is usually inactivated by epigenetic regulation (i.e., DNA methylation

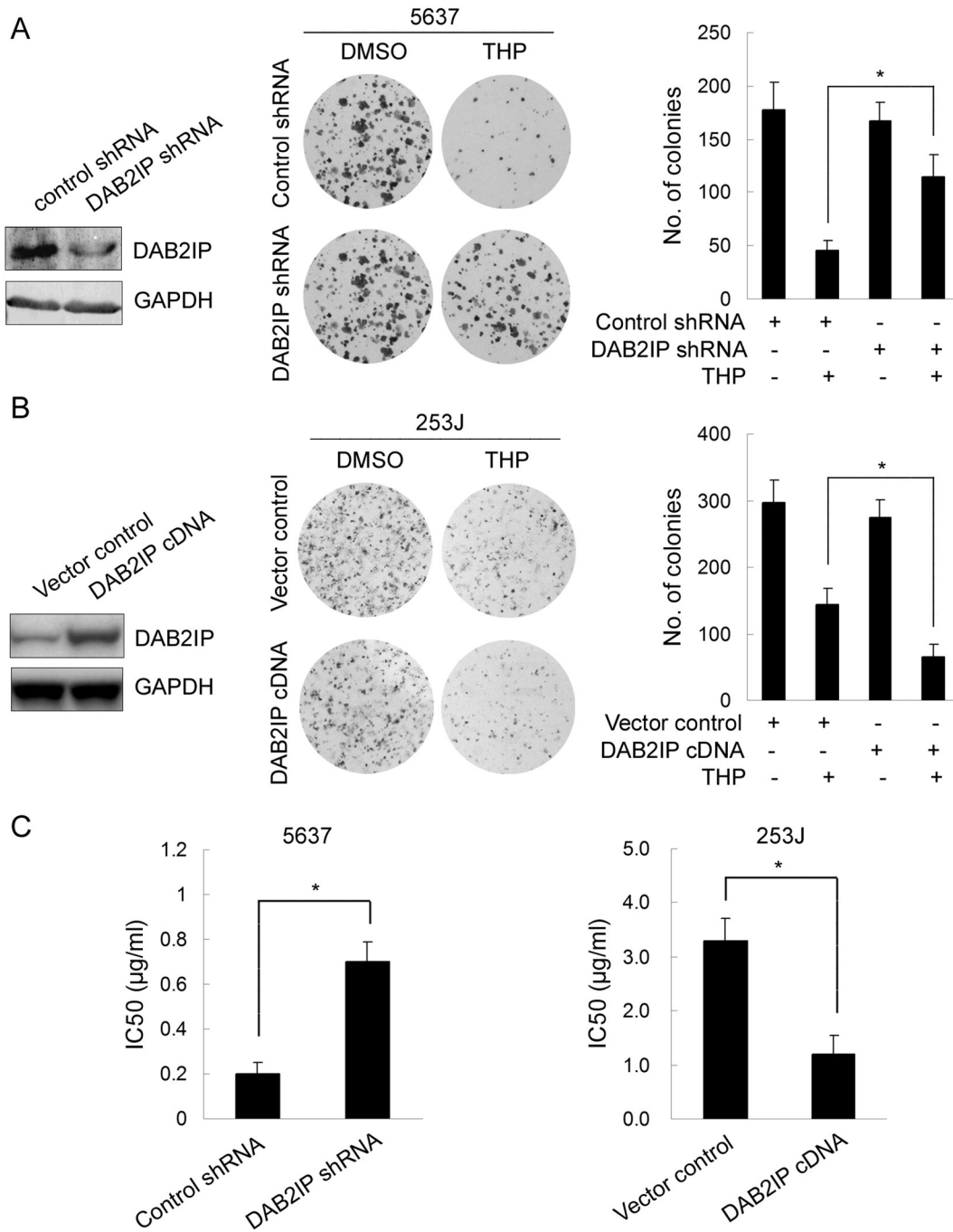


Fig. 2. DAB2IP regulates the chemosensitivity of BCa cells to pirarubicin treatment. A, 5637 cells were stably transfected with DAB2IP shRNAs or control shRNA. Left panel, the cell lysates were blotted with DAB2IP antibody and GAPDH was used as a loading control. Middle and right panel, 5637 sublines with 0.5 µg/ml THP treatment were subjected to colony formation assay, the representative pictures and quantification analysis of the colony formation after THP were shown, **P* < 0.05 vs. control. B, 253J cells were stably transfected with DAB2IP cDNA or vector control. Left panel, the cell lysates were blotted with DAB2IP antibody and GAPDH was used as a loading control. Middle and right panel, 5637 sublines with 0.5 µg/ml pirarubicin treatment were subjected to colony formation assay, the representative pictures and quantification analysis of the colony formation after THP treatment were shown, **P* < 0.05 vs. control. C, 5637 or 253J sublines were treated with different concentrations of THP, and then subjected to cell viability assay. IC50 of these sublines were calculated, and quantification analyses were shown, **P* < 0.05 vs. control.

and histone modification) or protein degradation in different human malignancies, such as prostate cancer [22], breast cancer [23], lung cancer [24], gastrointestinal tumor [25], liver cancer [26], pancreatic cancer [27], medulloblastoma [28] and esophageal carcinoma [29]. In addition, recent discoveries have outlined the important functions of this gene in cancer biology. It represents different tumor-suppressive roles in the regulation of cell apoptosis or survival [30], autophagy [31], DNA repair [32], EMT [13] and cancer stem cell (CSC) [33], all of which may contribute to the tumor initiation and progression. Similarly, our and other

groups have demonstrated that decreased DAB2IP expression is associated the clinicopathological features and poor outcomes in BCa patients, and it could regulate the biological behaviors of BCa cells through inactivation of MAPK and Akt pathways [6,7]. In this study, we further analyzed its expression pattern in the type of NMIBC, and reported that DAB2IP was also down-regulated in the high-grade or recurrent NMIBC tissues, and could modulate the in vitro and in vivo chemosensitivity of BCa cells to THP treatment, which was commonly used in NMIBC for intravesical instillation therapy after TUR in China.

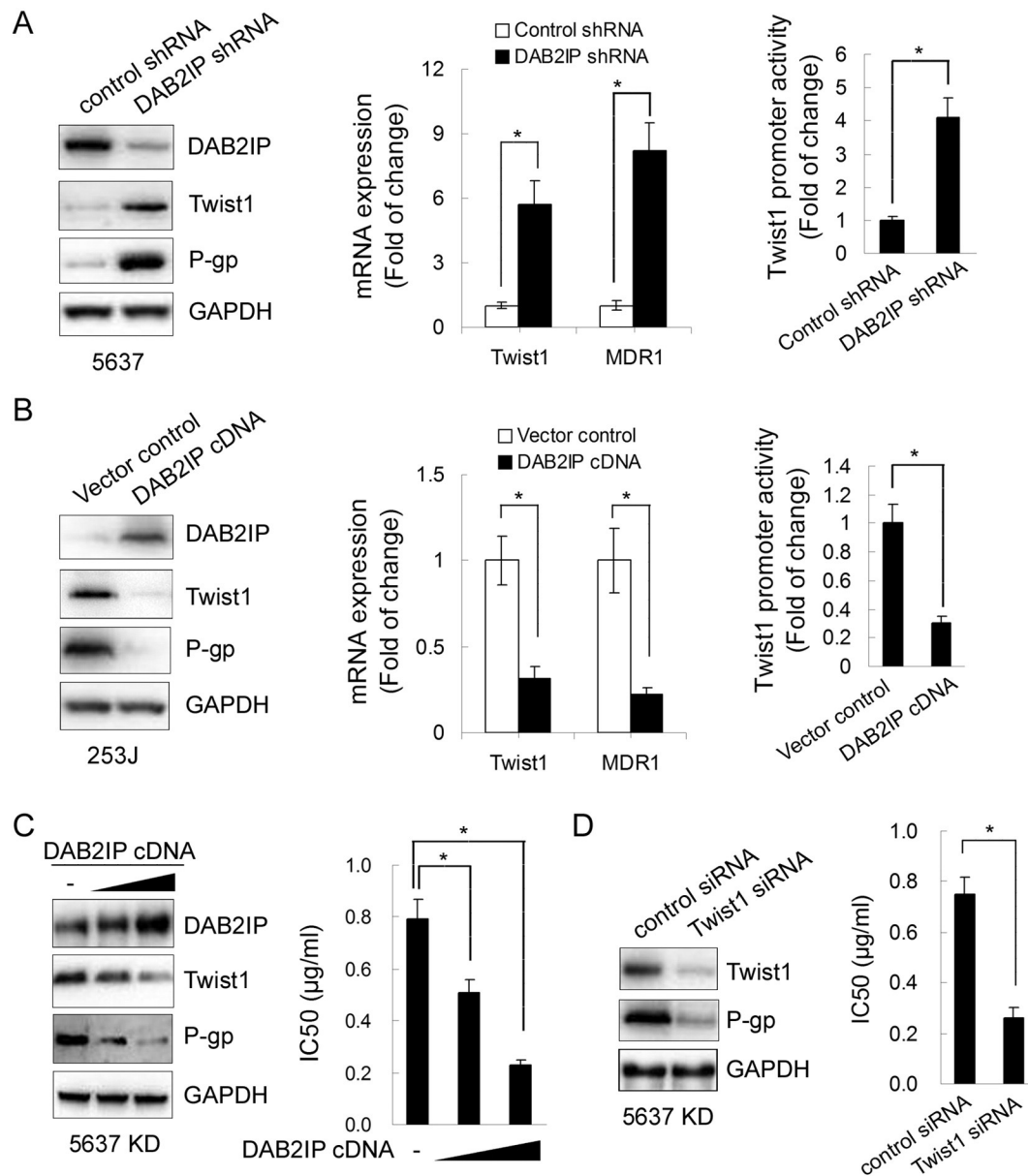


Fig. 3. DAB2IP controls the expression of Twist1 and P-gp to regulate the chemosensitivity of BCa cells. A–B, left panel, the cell lysates of 5637 or 253J sublines were blotted with DAB2IP, Twist1 or P-gp antibodies and GAPDH was used as a loading control; middle panel, Twist1 and MDR1 (P-gp) mRNA were detected in 5637 or 253J sublines by quantitative real-time RT-PCR. The relative mRNA level of each gene was determined by normalizing 18S rRNA. Results (mean \pm SEM) were obtained from three independent experiments. $^*P < 0.05$ vs. control; right panel, 5637 or 253J sublines were transfected with Twist1-luc and pRL-SV40 vectors for 48 h then reporter gene activities were determined using dual-luciferase assay. $^*P < 0.05$ vs. control. C, 5637 KD cells were transfected with different doses of DAB2IP expression vector. Left panel, the cell lysates were blotted with DAB2IP, Twist1 or P-gp antibodies and GAPDH was used as a loading control. Right panel, cells were treated with different concentrations of THP, and then subjected to cell viability assay. Quantification analyses of IC50 were shown, $^*P < 0.05$ vs. control. D, 5637 KD cells were transfected with Twist1 siRNA or control siRNA. Left panel, the cell lysates were blotted with Twist1 or P-gp antibodies and GAPDH was used as a loading control. Right panel, cells were treated with different concentrations of THP, and then subjected to cell viability assay. Quantification analyses of IC50 were shown, $^*P < 0.05$ vs. control.

Although the adjuvant intravesical chemotherapy or immunotherapy was recommended after TUR of NMIBC, the recurrence rate is still as high as 50–80% [34]. In general, the underlying mechanisms of chemoresistance are poorly understood. THP is an anthracycline derivative, which intercalates into DNA and interacts with topoisomerase II, thereby inhibiting DNA replication and repair, and RNA and protein synthesis. It has been shown to significantly decrease the risk of recurrence in patients with NMIBC as the neoadjuvant instillation of chemotherapy [35], but the efficacy of this chemotherapeutic agent remains controversial [36]. The ATP-dependent cellular efflux pump P-glycoprotein (P-gp, encoded by MDR1 gene) has been proved to participate in the chemoresistance by reducing intracellular concentration of chemotherapeutic drugs, including anthracyclines. Increased MDR1 gene

expression is frequently observed in recurrent or residual BCa tumors, and predict poor outcome of patients after chemotherapy [37,38]. In our previous study, we have reported that the basic helix–loop–helix transcription factor Twist1 could regulate P-gp expression and confer the chemoresistance of BCa cells to anthracycline [8]. Utilizing the same cell models, our further research showed that DAB2IP could modulate the chemoresistant phenotypes of BCa cells by suppressing this Twist1/P-gp axis.

Interestingly, a consistent change of the Twist1 protein and promoter activity was observed after we manipulated the DAB2IP expression levels in both 5637 and 253J cells, suggesting Twist1 as a potential downstream target gene of DAB2IP. Furthermore, we found that STAT3 mediated the regulation of Twist1 gene transcription by

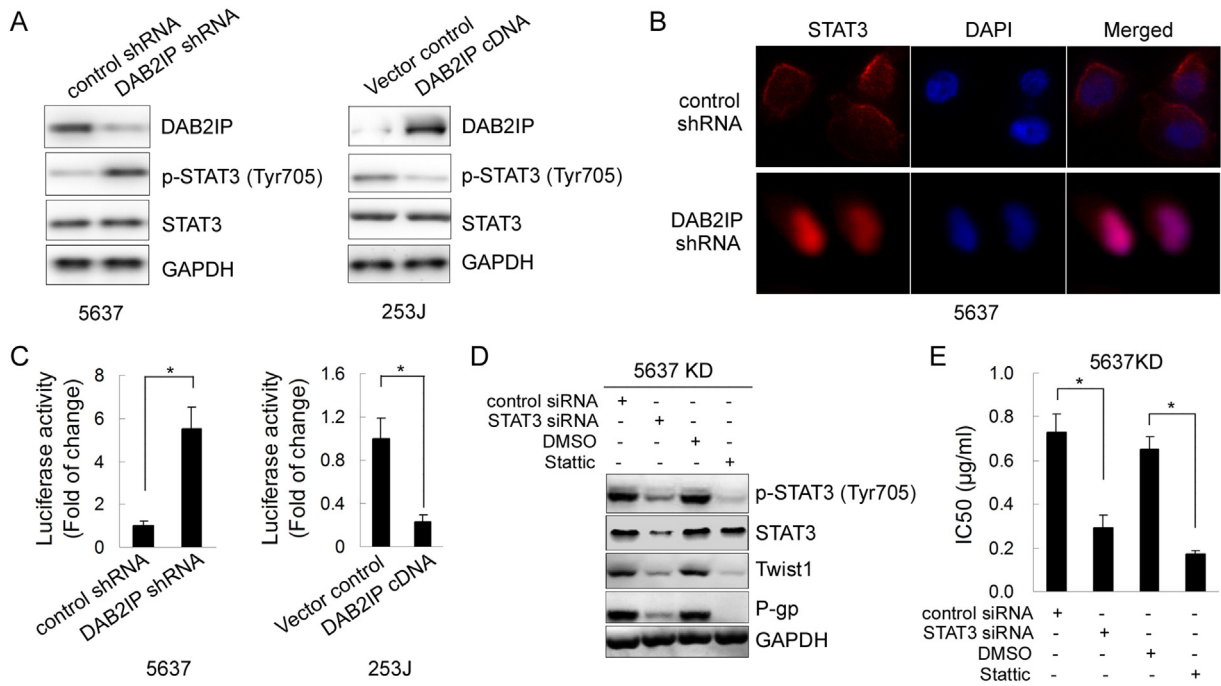


Fig. 4. STAT3 mediates the regulation of Twist1/P-gp expression and chemosensitivity by DAB2IP in BCa cells. A, the cell lysates of 5637 or 253J sublines were blotted with p-STAT3 (Tyr705) or STAT3 antibodies and DAPDH was used as a loading control; B, 5637 sublines were subjected to the immunofluorescence staining with STAT3 antibody (400×). C, 5637 or 253J sublines were transfected with pLucTKS3 and pRL-SV40 vectors for 48 h then reporter gene activities were determined using dual-luciferase assay. **P* < 0.05 vs. control. D, 5637 KD cells were transfected with STAT3 siRNA or treated with STAT3 inhibitor Stattic (10 µM). The cell lysates were blotted with p-STAT3 (Tyr705), STAT3, Twist1 or P-gp antibodies and GAPDH was used as a loading control. E, Cells after STAT3 siRNA transfection or Stattic pre-treatment were then treated with different concentrations of THP, and then subjected to cell viability assay. Quantification analyses of IC50 were shown, **P* < 0.05 vs. control.

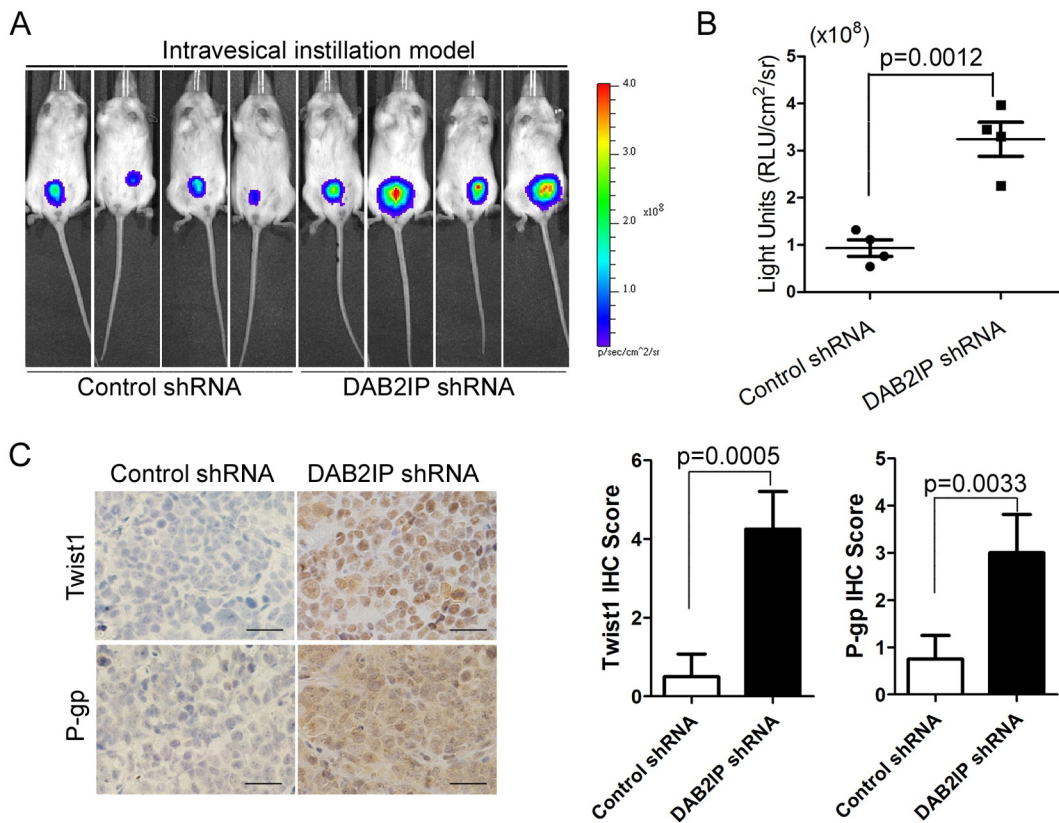


Fig. 5. DAB2IP-deficient BCa cells maintain an increased tumor growth after intravesical THP treatment in the orthotopic animal models. A, anesthetic female athymic BALB/c nu/nu mice were instilled with 100 µl medium containing 5×10^6 5637 sublines expressing luciferase into the bladder, and then treated with intravesical THP (30 mg/m²) instillation twice. The tumor burden was determined by BLI image, and the representative BLI images of live mice orthotopically instilled with 5637 sublines were shown after 3 weeks; B, quantification of light emission for orthotopic bladder cancer in mice after THP treatment was calculated; C, representative pictures of immunohistochemistry of Twist1 and P-gp in 5637 subline orthotopic xenograft tissues were shown. The scale bar represents 25 µm. Quantification analyses of IHC score were shown (right panel).

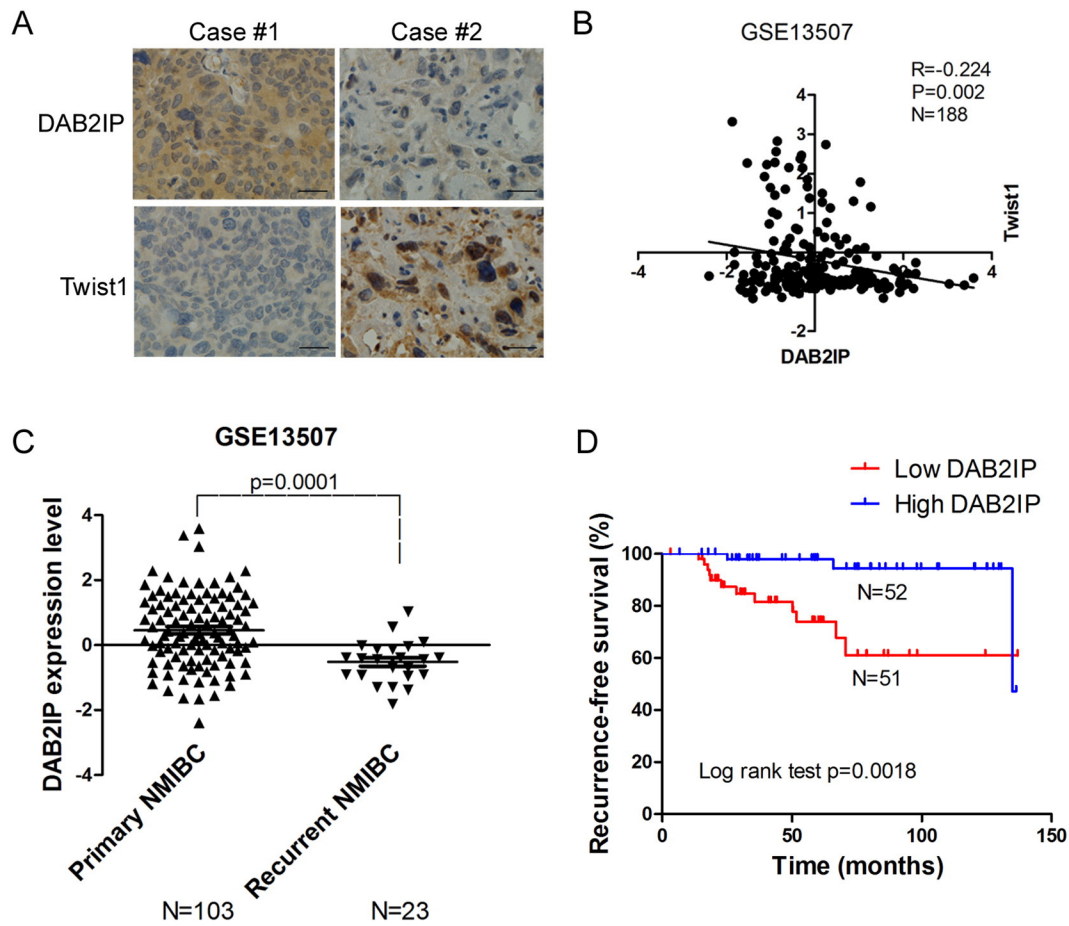


Fig. 6. Correlation between DAB2IP and Twist1 in human NMIBC tissues and its significance for patient prognosis. A, representative pictures of DAB2IP and Twist1 immunohistochemistry in NMIBC tissues were shown. The scale bar represents 25 μ m. B, correlation between DAB2IP and Twist1 mRNA in NMIBC tissues from a public available microarray database (GSE13507); C, decreased DAB2IP gene expression in human recurrent NMIBC ($n = 23$) compared with primary NMIBC ($n = 103$) from GSE13507 dataset analysis; D, percentage of recurrence-free survival was analyzed by Kaplan–Meier curves from GSE13507 dataset.

DAB2IP in our models since DAB2IP was not a typical transcription factor. Constitutive activation of STAT3 signaling pathway plays an important role in bladder cancer cell growth, survival, invasion and metastasis [39,40]. In our previous study, we have demonstrated that DAB2IP could interact with STAT3 protein and suppress its transcriptional activity in prostate cancer [17]. Herein, we further observed that DAB2IP could inhibit the phosphorylation, nuclear translocation and transactivation of STAT3 in BCa cells, which then subsequently repressed the Twist1 expression and sensitize BCa cells to THP treatment. This was consistent with other publication showing that STAT3 could directly bind to the Twist1 promoter and then activate its gene transcription [11,16,40,41]. In addition, the clinical data showed a decreased expression of DAB2IP in recurrent NMIBC specimens, and its loss predicted a poor recurrence-free survival rate of patients with NMIBC. Also, DAB2IP loss was significantly correlated with the expression of Twist1 in clinical tumor samples based on our IHC staining and analysis of gene microarray from other research group [15,18].

On the other hand, as we know, it is still hard to determine the sensitivity or resistance of chemotherapy in xenograft animal models due to the limitation of tumor real-time monitoring. In our previous studies, we have developed the bioluminescent imaging (BLI) to monitor the tumor growth in situ and spontaneous metastases after intravesical instillation of cancer cells [42]. Herein, we also successfully established the intravesical instillation xenograft models and applied this technique to detect the in situ tumor growth after THP treatment, and found that DAB2IP-deficient BCa cells acquired a survival advantage and developed

larger tumors compared with control. In consistency, these DAB2IP-deficient xenograft tumor tissues represented high expression levels of Twist1 and P-gp, supporting the critical roles of DAB2IP/Twist1/P-gp signaling axis in NMIBC tumor recurrence after THP chemotherapy in vivo.

Taken together, our studies reveal a novel role of DAB2IP in modulating the chemoresistance and tumor recurrence of NMIBC, in which STAT3 will regulate the expression of Twist1 and P-gp in vitro and in vivo. To be important, our findings provide a molecular and clinicopathological basis highlighting DAB2IP as a potential marker in prognosticating/predicting the outcome of NMIBC. Nevertheless, new markers hold the promise to be available tools for reliable risk assessment of NMIBC [19], which will represent a great advancement in counseling patients for selecting more effective adjuvant treatments.

Conflict of interest

The authors declare no conflict of interest.

Acknowledgments

This study was supported by the National Natural Science Foundation of China (NSFC 81572516 to KW; NSFC 81572520 JF) and the “13115” Scientific and Technological Innovation Project of Shaanxi Province, China (2008ZDKJ-63 to DH).

References

- [1] R.L. Siegel, K.D. Miller, A. Jemal, *CA Cancer J. Clin.* 65 (2015) 5–29.
- [2] M. Babjuk, M. Burger, R. Zigeuner, S.F. Shariat, B.W. van Rhijn, E. Comperat, R.J. Sylvester, E. Kaasinen, A. Böhle, J. Palou Redorta, M. Roupret, *Eur. Urol.* 64 (2013) 639–653.
- [3] M.P. Shekhar, *Curr. Cancer Drug Targets* 11 (2011) 613–623.
- [4] H. Chen, S. Toyooka, A.F. Gazdar, J.T. Hsieh, *J. Biol. Chem.* 278 (2003) 3121–3130.
- [5] E. Kunze, F. Von Bonin, C. Werner, M. Wendt, T. Schlott, *Int. J. Mol. Med.* 17 (2006) 3–13.
- [6] Y.J. Shen, Z.L. Kong, F.N. Wan, H.K. Wang, X.J. Bian, H.L. Gan, C.F. Wang, D.W. Ye, *Cancer Sci.* 105 (2014) 704–712.
- [7] J.N. Zhu, K.J. Wu, Z.F. Guan, L.X. Liu, Z.Y. Ning, J.C. Zhou, X.Y. Wang, J.H. Fan, *Sichuan Da Xue Xue Bao Yi Xue Ban* 45 (2014) 591–594.
- [8] Y. Chen, L. Li, J. Zeng, K. Wu, J. Zhou, P. Guo, D. Zhang, Y. Xue, L. Liang, X. Wang, L.S. Chang, D. He, *Chemotherapy* 58 (2012) 264–272.
- [9] Z. Wang, C.P. Tseng, R.C. Pong, H. Chen, J.D. McConnell, N. Navone, J.T. Hsieh, *J. Biol. Chem.* 277 (2002) 12622–12631.
- [10] K. Wu, D. Xie, Y. Zou, T. Zhang, R.C. Pong, G. Xiao, L. Fazli, M. Gleave, D. He, D.A. Boothman, J.T. Hsieh, *Clin. Cancer Res.* 19 (2013) 4740–4749.
- [11] G.Z. Cheng, W.Z. Zhang, M. Sun, Q. Wang, D. Coppola, M. Mansour, L.M. Xu, C. Costanzo, J.Q. Cheng, L.H. Wang, *J. Biol. Chem.* 283 (2008) 14665–14673.
- [12] Z.G. Dikmen, G.C. Gellert, S. Jackson, S. Gryaznov, R. Tressler, P. Dogan, W.E. Wright, J.W. Shay, *Cancer Res.* 65 (2005) 7866–7873.
- [13] D. Xie, C. Gore, J. Liu, R.C. Pong, R. Mason, G. Hao, M. Long, W. Kabbani, L. Yu, H. Zhang, H. Chen, X. Sun, D.A. Boothman, W. Min, J.T. Hsieh, *Proc. Natl. Acad. Sci. U. S. A.* 107 (2010) 2485–2490.
- [14] G. Zhu, H.E. Zhou, H. He, L. Zhang, B. Shehata, X. Wang, W.H. Cerwinka, J. Elmore, D. He, *Prostate* 67 (2007) 674–684.
- [15] J.S. Lee, S.H. Leem, S.Y. Lee, S.C. Kim, E.S. Park, S.B. Kim, S.K. Kim, Y.J. Kim, W.J. Kim, I.S. Chu, *J. Clin. Oncol.* 28 (2010) 2660–2667.
- [16] A. Takeuchi, M. Shiota, E. Beraldi, D. Thaper, K. Takahara, N. Ibuki, M. Pollak, M.E. Cox, S. Naito, M.E. Gleave, A. Zoubeidi, *Mol. Cell. Endocrinol.* 384 (2014) 117–125.
- [17] J. Zhou, Z. Ning, B. Wang, E.-J. Yun, T. Zhang, R.-C. Pong, L. Fazli, M. Gleave, J. Zeng, J. Fan, X. Wang, L. Li, J.-T. Hsieh, D. He, K. Wu, *Cell Death Dis.* (2015).
- [18] W.J. Kim, E.J. Kim, S.K. Kim, Y.J. Kim, Y.S. Ha, P. Jeong, M.J. Kim, S.J. Yun, K.M. Lee, S.K. Moon, S.C. Lee, E.J. Cha, S.C. Bae, *Mol. Cancer* 9 (2010) 3.
- [19] L.A. Kluth, P.C. Black, B.H. Bochner, J. Catto, S.P. Lerner, A. Stenzl, R. Sylvester, A.J. Vickers, E. Xylinas, S.F. Shariat, *Eur. Urol.* 68 (2015) 238–253.
- [20] W. Choi, S. Porten, S. Kim, D. Willis, E.R. Plimack, J. Hoffman-Censits, B. Roth, T. Cheng, M. Tran, I.L. Lee, J. Melquist, J. Bondaruk, T. Majewski, S. Zhang, S. Pretzsch, K. Baggerly, A. Siefker-Radtke, B. Czerniak, C.P. Dinney, D.J. McConkey, *Cancer Cell* 25 (2014) 152–165.
- [21] N. Frstrup, B.P. Ulhøi, K. Birkenkamp-Demtroder, F. Mansilla, M. Sanchez-Carbayo, U. Segersten, P.U. Malmström, A. Hartmann, J. Palou, M. Alvarez-Mugica, K. Zieger, M. Borre, T.F. Orntoft, L. Dyrskjot, *Am. J. Pathol.* 180 (2012) 1824–1834.
- [22] H. Chen, R.C. Pong, Z. Wang, J.T. Hsieh, *Genomics* 79 (2002) 573–581.
- [23] H. Dote, S. Toyooka, K. Tsukuda, M. Yano, M. Ouchida, H. Doihara, M. Suzuki, H. Chen, J.T. Hsieh, A.F. Gazdar, N. Shimizu, *Clin. Cancer Res.* 10 (2004) 2082–2089.
- [24] M. Yano, S. Toyooka, K. Tsukuda, H. Dote, M. Ouchida, T. Hanabata, M. Aoe, H. Date, A.F. Gazdar, N. Shimizu, *Int. J. Cancer* 113 (2005) 59–66.
- [25] H. Dote, S. Toyooka, K. Tsukuda, M. Yano, T. Ota, M. Murakami, M. Naito, M. Toyota, A.F. Gazdar, N. Shimizu, *Br. J. Cancer* 92 (2005) 1117–1125.
- [26] D.F. Calvisi, S. Ladu, E.A. Conner, D. Seo, J.T. Hsieh, V.M. Factor, S.S. Thorgeirsson, *J. Hepatol.* 54 (2011) 311–319.
- [27] Y.F. Duan, D.F. Li, Y.H. Liu, P. Mei, Y.X. Qin, L.F. Li, Q.X. Lin, Z.J. Li, *Hepatobiliary Pancreat. Dis. Int.* 12 (2013) 204–209.
- [28] M. Smits, S. van Rijn, E. Hulleman, D. Biesmans, D.G. van Vuurden, M. Kool, C. Haberler, E. Aronica, W.P. Vandertop, D.P. Noske, T. Wurdinger, *Clin. Cancer Res.* 18 (2012) 4048–4058.
- [29] Y. Xu, J. He, Y. Wang, X. Zhu, Q. Pan, Q. Xie, F. Sun, *FEBS Lett.* 589 (2015) 1127–1135.
- [30] D. Xie, C. Gore, J. Zhou, R.C. Pong, H. Zhang, L. Yu, R.L. Vessella, W. Min, J.T. Hsieh, *Proc. Natl. Acad. Sci. U. S. A.* 106 (2009) 19878–19883.
- [31] L. Yu, V. Tumati, S.F. Tseng, F.M. Hsu, D.N. Kim, D. Hong, J.T. Hsieh, C. Jacobs, P. Kapur, D. Saha, *Neoplasia* 14 (2012) 1203–1212.
- [32] Z. Kong, D. Xie, T. Boike, P. Raghavan, S. Burma, D.J. Chen, A.A. Habib, A. Chakraborty, J.T. Hsieh, D. Saha, *Cancer Res.* 70 (2010) 2829–2839.
- [33] E.J. Yun, S.T. Baek, D. Xie, S.F. Tseng, T. Dobin, E. Hernandez, J. Zhou, L. Zhang, J. Yang, H. Sun, G. Xiao, D. He, R. Kittler, J.T. Hsieh, *Oncogene* 34 (2015) 2741–2752.
- [34] K.H. Kurth, C. Bouffloux, R. Sylvester, A.P. van der Meijden, W. Oosterlinck, M. Brausi, *Eur. Urol.* 37 (Suppl 3) (2000) 1–9.
- [35] H. Akaza, T. Nijima, T. Hisamatsu, M. Fujigaki, *Urology* 32 (1988) 141–145.
- [36] A. Pawinski, R. Sylvester, K.H. Kurth, C. Bouffloux, A. van der Meijden, M.K. Parmar, L. Bijns, *J. Urol.* 156 (1996) 1934–1940 discussion 1940–1931.
- [37] S. Hasegawa, T. Abe, S. Naito, S. Kotoh, J. Kumazawa, D.R. Hipfner, R.G. Deeley, S.P. Cole, M. Kuwano, *Br. J. Cancer* 71 (1995) 907–913.
- [38] A.C. Hoffmann, P. Wild, C. Leicht, S. Bertz, K.D. Danenberg, P.V. Danenberg, R. Stohr, M. Stockle, J. Lehmann, M. Schuler, A. Hartmann, *Neoplasia* 12 (2010) 628–636.
- [39] C.L. Chen, L. Cen, J. Kohout, B. Hutzen, C. Chan, F.C. Hsieh, A. Loy, V. Huang, G. Cheng, J. Lin, *Mol. Cancer* 7 (2008) 78.
- [40] D. Zhao, A.H. Besser, S.A. Wander, J. Sun, W. Zhou, B. Wang, T. Ince, M.A. Durante, W. Guo, G. Mills, D. Theodorescu, J. Slingerland, *Oncogene* (2015).
- [41] K.H. Cho, K.J. Jeong, S.C. Shin, J. Kang, C.G. Park, H.Y. Lee, *Cancer Lett.* 336 (2013) 167–173.
- [42] K. Wu, Z. Ning, J. Zeng, J. Fan, J. Zhou, T. Zhang, L. Zhang, Y. Chen, Y. Gao, B. Wang, P. Guo, L. Li, X. Wang, D. He, *Cell. Signal.* 25 (2013) 2625–2633.